PAD	VSWR		Attenuation of Pad	Attenuation of Pad and Tuners	Actual Reduction	Expected Reduction
	Male End	Female End				
A	1.75	1.54	7.368 DB	7.166 DB	.202 DB	0.3-0.9 DB
B	1 14	1 08	6.776 DB	7.079	-.303	.01-.04 DB
C	1.32	1.06	10 392 DB	10.641	-.249	.14-.18 DB

Fig. 4—Expected vs actual reduction in attenuation for coaxial pads measured at 4 Gc.

formers in rectangular waveguide in which there is no dielectric support required for the center conductor. Also it is apparent that tuning for bilateral match can be worthwhile when the degree of mismatch is large (VSWR > 2).

Conclusions

It was noted that "insertion loss" in general depends not only upon the parameters of the network, but also upon the characteristics of the system into which it is inserted. Hence the minimum insertion loss of a network cannot in general be regarded as intrinsic to the network, and the term "intrinsic attenuation" is recommended. Formulas were given to permit calculation of this quantity, given the scattering coefficients of the network. A graph was presented to rapidly estimate the reduction in attenuation to be expected when tuning a symmetrical attenuator for bilateral match, given only the attenuation and VSWR of the attenuator. The significance of tuning for bilateral match was explained, and a method given for obtaining this condition. Experimental results indicated that in the case of mismatched attenuators, little or nothing is to be gained when tuning for bilateral match, and, in some cases, the losses in the tuning transformers may cause a net increase in loss, rather than a reduction. However, in a situation in which the degree of mismatch is large (VSWR > 2), a significant decrease in loss should be obtained when tuning for the bilateral nonreflecting matched condition.

Acknowledgment

Calculations for the graph of Fig. 3 were performed by W. A. Downing, Jr. Measurements for Fig. 4 were performed by W. E. Little.

Analytical Solution to a Waveguide Leaky-Wave Filter Structure*

EDWARD G. CRISTAL†, MEMBER, IEEE

Summary—**Leaky-wave absorption filters have been found advantageous for the suppression of spurious energy of high-power transmitters. However, although there are experimental data of the properties of several specially constructed leaky-wave filters, there are apparently little data relating the effect upon the attenuation of the filters of varying one or more of the possible parameters of their design. In this paper a waveguide leaky-wave filter structure that retains the basic geometry of waveguide leaky-wave filters is analyzed theoretically over a finite frequency range. The complex propagation constant for the least-attenuated leaky-wave mode is obtained by reducing the fundamental integral equation to a transverse resonance equation and solving the reduced equation. The attenuation constant of the least-attenuated mode is obtained for values of $2a/\lambda$ (*i.e.*, the ratio of waveguide width to one half the free-space wavelength) ranging from 0 to 2. Its dependence on various design parameters of leaky-wave filters, such as main waveguide height, spacing of the coupling slots, width of coupling slots and height of the absorbing waveguides is presented. Good correspondence between theoretically computed curves and experimental data was obtained.**

* Received October 1, 1962; revised manuscript received January 18, 1963. The work reported here was sponsored by the Air Force Systems Command, Rome Air Development Center, Griffiss Air Force Base, New York, N. Y., under Contract No. AF 30(602)-2734.

† Standard Research Institute, Menlo Park, Calif.

Introduction

In recent years waveguide structures that support leaky-wave modes[1,2] have been found advantageous for the suppression of spurious energy of high-power transmitters. These structures are generally referred to as leaky-wall or leaky-wave filters.[3–5] They are absorption rather than reflection filters and exhibit the following characteristics:

1) They generally provide high attenuation throughout a wide stop band.

[1] N. Marcuvitz, "On field representations in terms of leaky modes or eigenmodes," IRE Trans. on Antennas and Propagation, vol. AP-4, pp. 192–194; July, 1956.

[2] K. G. Budden, "The Wave-Guide Mode Theory of Wave Propagation," Prentice-Hall, Inc., Englewood Cliffs, N. J., pp. 4, 134; 1961.

[3] V. Met, "Absorptive filters for microwave harmonic power," Proc. IRE, vol. 47, pp. 1762–1769; October, 1959.

[4] V. Price, R. Stone and V. Met, "Harmonic Suppression by Leaky-Wall Waveguide Filter," 1959 IRE Wescon Convention Record, pt. 1, pp. 112–116.

[5] E. G. Cristal, "Some preliminary experimental results on coaxial absorption leaky-wave filters," *4th Ann. Symp. on Radio Frequency Interference*, San Francisco, Calif., June 28–29, 1962.

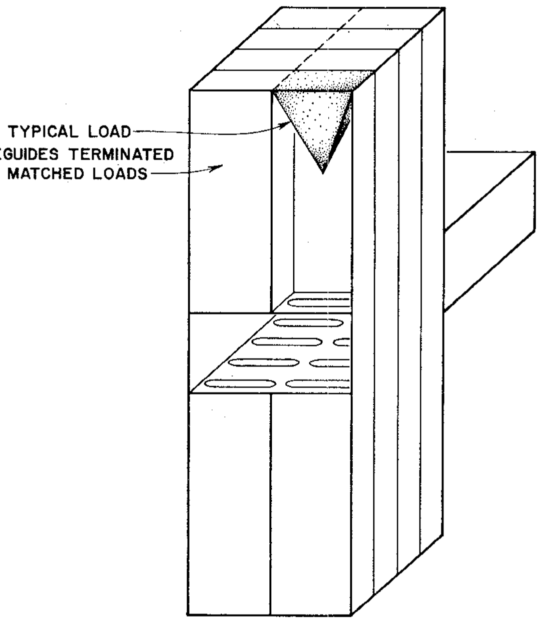

Fig. 1—Sketch of a possible type of waveguide leaky-wave filter.

2) They are reasonably well matched to the transmitter in the stop band as well as the pass band.
3) They are able to support large peak power levels.

Because of these properties it is expected that leaky-wave filters will play an important part in the suppression of spurious energy, particularly in view of the anticipated increased crowding of the radio spectrum, the development of more sensitive receivers and the expected greater power output of new transmitting tubes.[6] Consequently, there is a need for a greater understanding of these filters and for quantitative data regarding their design.

Although there are experimental data on the properties of several specially constructed leaky-wave filters,[5,7,8] there are apparently little data relating the effect on the attenuation of the filters of varying one or more of the possible parameters of their design. It is the intent of the present analysis to consider this particular aspect theoretically over a limited frequency range.

Basically, leaky-wave filters consist of a transmission line that is modified by having closely spaced periodic slots cut on the walls (outer wall for coaxial leaky-wave filters). Each slot couples the transmission line to a waveguide that is terminated in a wideband matched load. At frequencies in the filter pass band, the side waveguides are cut off and the energy in the transmission line passes to the output unattenuated. However,

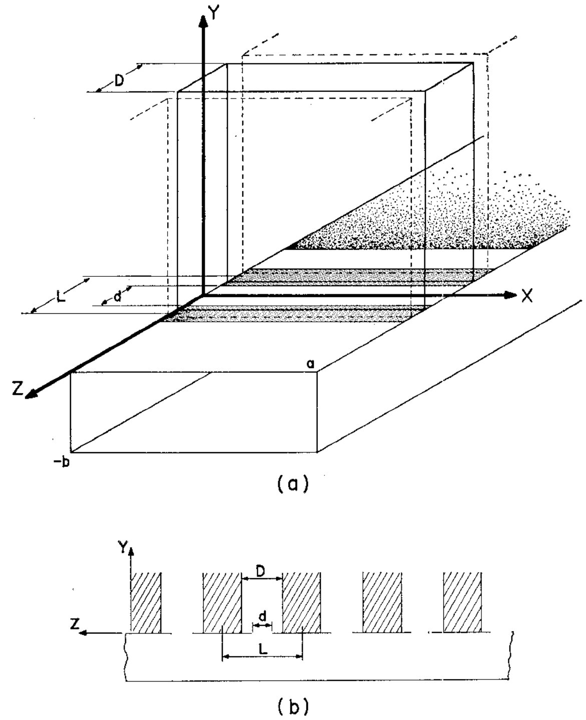

Fig. 2—Waveguide leaky-wave filter structure. (a) Orthogonal projection. (b) Longitudinal-section view.

at frequencies in the filter stop band, the side waveguides support propagation and hence the energy at these frequencies is coupled into the absorbing waveguides and is thus severely attenuated. A sketch of one possible type of waveguide leaky-wave filter is shown in Fig. 1.

These structures are not readily amenable to a theoretical study; for this reason, an idealized structure, which, however, retains the basic geometry of a leaky-wave filter, will be used for this analysis. The structure is shown in Fig. 2. It consists of a waveguide that has closely spaced periodic slots cut in one of the broad walls. Each slot looks into a single side waveguide that is assumed to be terminated in its characteristic impedance. As can be perceived from Fig. 2(a), this structure has no pass band since both the main transmission line and side waveguides have the same cutoff frequencies. Nevertheless, the analysis which follows is believed to be pertinent to leaky-wave filter design for the following reasons:

1) Assume a TE_{20} mode incident to the leaky-wave filter of Fig. 1. Then, from the symmetry of the structure and the mode of excitation, it can be seen that a conducting (electric) wall could be placed in the E plane between the slots without disturbing the fields. If this were done, the resulting configuration would bear a very close resemblence to the structure of Fig. 2(a). Thus, the results obtained from the analysis may provide useful quantitative data for the attenuation of this mode. A similar argument applies for filters having 3 slots abreast on the broad wall and in-

[6] O. M. Salati, "Recent developments in RF interference," IRE Trans. on Radio Frequency Interference, vol. RFI-4, pp. 24–32; May, 1962.
[7] V. G. Price, J. P. Rooney and C. Milazzo, "Measurement and Control of Harmonic and Spurious Microwave Energy, Final Report for Phase II," G. E. Microwave Lab., Palo Alto, Calif., Rept. No. TISR58ELM 112-1, Contract No. AF 30(602)-1670; 1958.
[8] V. G. Price, J. P. Rooney and R. H. Stone, "Measurement and Control of Harmonic and Spurious Microwave Energy, Final Report Change A," G. E. Microwave Lab., Palo Alto, Calif., Rept. No. TIS60ELM 112-4, Contract No. AF 30(602)-1670; 1960.

cident TE_{30} modes, or for n slots abreast on the broad wall and incident TE_{n0} modes.

2) In the frequency intervals where the coupling slots of practical leaky-wave filters are past resonance, their frequency dependence is similar to that of the capacitive slots of the structure in Fig. 2(a). Also, the frequency dependence of the absorbing waveguides for both cases is similar. Therefore, it is believed that while the quantitative data resulting from this analysis may not apply directly to actual leaky-wave filters propagating the TE_{10} mode, the dependence of the attenuation constant on the various design parameters will behave in the same general way. Hence, which parameters should be varied to maximize the attenuation constant, or to make it less frequency sensitive, can be ascertained from this work.

3) The analysis can easily be extended by symmetry considerations to the case where slots are cut on both broad walls.

4) The analysis of the periodic structure automatically accounts for all mutual coupling effects of the slots.

Derivation of the Integral Equation for the Determination of Leaky-Wave Modes

Referring to Figs. 2(a) and (b), we assume transmission in the z direction in a waveguide of width a and height b. The slots on the broad wall extend across the total width of the guide and are of width d. They are located at periods of length L. The side waveguides are also of width a, but are of variable height D. Because of the limitations imposed by the geometry, their heights may range from d to L, but in all cases will be assumed the same for all guides. Because of the periodic nature of the structure, we may assume propagation to be of the form

$$e^{-\Gamma_n z},$$

where

$$\Gamma_n = \gamma_z + j\frac{2\pi n}{L},$$

$$\gamma_z = \alpha + j\beta. \tag{1}$$

The procedure for obtaining the propagation constant γ_z follows. Assuming that the exciting wave is a TE_{10} mode incident from a tandem section of regular guide, the lowest order permissible modes in the main transmission waveguide are the longitudinal-section electric (LSE) modes.[9] With respect to the coordinate system shown in Fig. 2(a) the fields in the main guide are given by (2).

$$E_z = \sum_{n=-\infty}^{\infty} A_n \sinh \gamma_n(y+b) \sin\left(\frac{\pi}{a}x\right) e^{-\Gamma_n z}$$

$$E_y = \sum_{n=-\infty}^{\infty} \frac{A_n}{\gamma_n} \Gamma_n \cosh \gamma_n(y+b) \sin\left(\frac{\pi}{a}x\right) e^{-\Gamma_n z}$$

$$H_z = \sum_{n=-\infty}^{\infty} -\frac{(\pi/a)\Gamma_n}{j\omega\mu\gamma_n} A_n \cosh \gamma_n(y+b) \cos\left(\frac{\pi}{a}x\right) e^{-\Gamma_n z}$$

$$H_y = \sum_{n=-\infty}^{\infty} \frac{(\pi/a)}{j\omega\mu} A_n \sinh \gamma_n(y+b) \cos\left(\frac{\pi}{a}x\right) e^{-\Gamma_n z}$$

$$H_x = \sum_{n=-\infty}^{\infty} -Y_n A_n \cosh \gamma_n(y+b) \sin\left(\frac{\pi}{a}x\right) e^{-\Gamma_n z}$$

$$K^2 = (\pi/a)^2 - k^2$$

$$k = \frac{2\pi}{\lambda}$$

$$\gamma_n^2 = K^2 - \Gamma_n^2$$

$$Y_n = \frac{(\pi/a)^2 - k^2}{j\omega\mu\gamma_n} = \frac{K^2}{j\omega\mu\gamma_n}. \tag{2}$$

Assuming that the side waveguides are terminated in their characteristic impedances, their fields are given by (3)

$$E_z = \sum_{n=0}^{\infty} B_n \cos\frac{n2\pi}{D} z \sin\frac{\pi}{a} x\, e^{-\gamma_{yn} y}$$

$$E_y = \sum_{n=1}^{\infty} -\frac{(n2\pi/D)}{\gamma_{yn}} B_n \sin\frac{n2\pi}{D} z \sin\left(\frac{\pi}{a}x\right) e^{-\gamma_{yn} y}$$

$$H_z = \sum_{n=1}^{\infty} \frac{(n2\pi/D)(\pi/a)}{j\omega\mu\gamma_{yn}} B_n \sin\frac{n2\pi}{D} z \cos\left(\frac{\pi}{a}x\right) e^{-\gamma_{yn} y}$$

$$H_y = \sum_{n=0}^{\infty} \frac{(\pi/a)}{j\omega\mu} B_n \cos\frac{n2\pi}{D} z \cos\left(\frac{\pi}{a}x\right) e^{-\gamma_{yn} y}$$

$$H_x = \sum_{n=0}^{\infty} y_n B_n \cos\frac{n2\pi}{D} z \sin\left(\frac{\pi}{a}x\right) e^{-\gamma_{yn} y}$$

$$\gamma_{yn}^2 = K^2 + \left(\frac{n2\pi}{D}\right)^2$$

$$y_n = \frac{(\pi/a)^2 - k^2}{j\omega\mu\gamma_{yn}} = \frac{K^2}{j\omega\mu\gamma_{yn}}. \tag{3}$$

Denote the tangential electric field in the coupling gap as $E(z)$. Then

$$E_z(x, 0, z) = \begin{cases} E(z) & 0 \le x \le a;\ \frac{-d}{2} < z < \frac{d}{2} \\ 0 & 0 \le x \le a;\ \frac{d}{2} \le |z| \le \frac{L}{2}. \end{cases} \tag{4}$$

[9] R. E. Collin, "Field Theory of Guided Waves," McGraw-Hill Book Company, Inc., New York, N. Y., p. 225; 1960.

The coefficients A_n and B_n of (2) and (3) are

$$A_n = \frac{1}{L \sinh \gamma_n b} \int_{-d/2}^{d/2} E(u) e^{\Gamma_n u} du,$$
$$B_n = \frac{\epsilon_n}{D} \int_{-d/2}^{d/2} E(u) \cos \frac{n 2\pi u}{D} du,$$
$$\epsilon_n = \left.\begin{matrix} 1 \\ 2 \end{matrix}\right\} \quad \begin{matrix} n = 0 \\ n \neq 0 \end{matrix}. \tag{5}$$

Substituting these expressions for the coefficients A_n and B_n of (2) and (3) the field expressions become explicit functions of the tangential electric field in the coupling gap. In particular, in the main transmission line,

$$H_x = -\frac{1}{L} \sum_{n=-\infty}^{\infty} Y_n \frac{\cosh \gamma_n (y + b)}{\sinh \gamma_n b} du \cdot \int_{-d/2}^{d/2} E(u) e^{\Gamma_n u} du e^{-\Gamma_n z} \sin \frac{\pi}{a} x,$$

and in the side waveguide,

$$H_x = \frac{1}{D} \sum_{n=0}^{\infty} \epsilon_n y_n \cos \frac{n 2\pi}{D} z \int_{-d/2}^{d/2} E(u) \cos \frac{n 2\pi u}{D} du \cdot \sin\left(\frac{\pi}{a} x\right) e^{-\gamma_{yn} y}. \tag{6}$$

In order that the tangential magnetic field be continuous in the gap, the equations of (6) must be identically equal at $y=0$. Equating the two expressions when $y=0$ and interchanging the order of integration and summation gives the following integral equation for the determination of the propagation constant.

$$\int_{-d/2}^{d/2} E(u) G(\gamma_z, u, z)\, du \equiv 0$$

where

$$G(\gamma_z, u, z) = \frac{1}{L} \sum_{n=-\infty}^{\infty} Y_n (\coth \gamma_n b) e^{\Gamma_n (u-z)} + \frac{1}{D} \sum_{n=0}^{\infty} \epsilon_n y_n \cos \frac{n 2\pi u}{D} \cos \frac{n 2\pi}{D} z. \tag{7}$$

Since the advent of large, very fast, electronic computers, it is possible to solve (7) by straightforward numerical techniques. However, in the present problem, by using suitable approximations and known handbook expressions, (7) may be reduced to a more simple transverse resonance equation.[10,11]

Reduction of the Integral Equation to a Transverse Resonance Equation

By multiplying (7) by $E(z)$, integrating with respect to z from $-d/2$ to $d/2$ and rearranging terms, (7) may be put in the form

$$\frac{Y_0}{L} \coth \gamma_0 b = - \frac{\left\{ \frac{1}{L} \sum_{\substack{n=-\infty \\ n \neq 0}}^{\infty} Y_n \coth \gamma_n b \int_{-d/2}^{d/2} E(u) e^{\Gamma_n u} du \int_{-d/2}^{d/2} E(z) e^{-\Gamma_n z} dz + \frac{y_0}{D} \int_{-d/2}^{d/2} E(u) du \int_{-d/2}^{d/2} E(z) dz + \frac{2}{D} \sum_{n=1}^{\infty} \int_{-d/2}^{d/2} E(u) \cos \frac{2\pi n}{D} u du \int_{-d/2}^{d/2} E(z) \cos \frac{2\pi n z}{D} dz \right\}}{\int_{-d/2}^{d/2} E(u) e^{\Gamma_0 u} du \int_{-d/2}^{d/2} E(z) e^{-\Gamma_0 z} dz}. \tag{8}$$

Eq. (8) is exact and is satisfied by the proper $E(u)$ and γ_z. However, considerable simplification can be achieved by making the following approximations:

Assume that

$$\left.\begin{matrix} \beta + \frac{2\pi n}{L} \gg \alpha \\ \frac{2\pi n}{L} \gg \beta \end{matrix}\right\} \quad \text{for } n \geq 1. \tag{9}$$

Then it follows that

$$\Gamma_n \approx \left(j \frac{2\pi n}{L}\right) \quad \text{for } n \geq 1, \tag{10}$$

$$Y_n \approx \frac{K^2}{j\omega\mu \sqrt{K^2 + \left(\frac{2\pi n}{L}\right)^2}} \quad \text{for } n \geq 1, \tag{11}$$

and

$$\coth \gamma_n b \approx \coth b \sqrt{K^2 + \left(\beta + \frac{2\pi n}{L}\right)^2}. \tag{12}$$

For the range of parameters that will be considered it is true that

$$b \sqrt{K^2 + \left(\beta + \frac{2\pi n}{L}\right)^2} \gg 3. \tag{13}$$

Therefore,

$$\coth \gamma_n b \approx 1. \tag{14}$$

[10] L. O. Goldstone and A. A. Oliner, "Leaky-wave antennas I: rectangular waveguides," IRE Trans. on Antennas and Propagation, vol. AP-7, pp. 307–319; October, 1959.

[11] R. C. Honey, "Horizontally Polarized Long-Slot Array, Stanford Research Inst., Menlo Park, Calif., Tech. Rept. No. 47, SRI Project 591, Air Force Contract No. AF 19(604)-266; 1954.

Also we assume that on the square

$$\frac{-d}{2} \le u \le \frac{d}{2}$$
$$\frac{-d}{2} \le z \le \frac{d}{2} \tag{15}$$

the expression $\Gamma_0(u-z)$ satisfies the inequality

$$|\Gamma_0(u-z)| \ll 1. \tag{16}$$

As a result of the inequality (16) we make the approximation

$$e^{\Gamma_0(u-z)} \approx 1. \tag{17}$$

With due consideration to approximations (10), (11), (14) and (17)[12] (8) may be rewritten as

$$\coth \gamma_0 b \approx - \frac{\left\{ 2 \sum_{n=1}^{\infty} \frac{y_n}{Y_0} \int_{-d/2}^{d/2} \int_{-d/2}^{d/2} E(u)E(z) \cos \frac{2\pi n}{L} u \cos \frac{2\pi n}{L} z du dz + 2 \frac{L}{D} \sum_{n=1}^{\infty} \frac{Y_n}{Y_0} \int_{-d/2}^{d/2} \int_{-d/2}^{d/2} E(u)E(z) \cos \frac{2\pi n}{D} u \cos \frac{2\pi n}{D} z du dz \right\}}{\int_{-d/2}^{d/2} \int_{-d/2}^{d/2} E(u)E(z) du dz} + \frac{L\gamma_0}{DH}. \tag{18}$$

Comparing the first and second terms of (18) with analogous variational expressions in Collin,[13] we conclude that (7) is approximated by the following transverse resonance equation:

$$\coth \gamma_0 b \approx - \gamma_0 \left\{ \frac{L/D}{H} + \frac{L}{\pi} \ln \csc \frac{\pi}{2} \frac{d}{L} + \frac{L}{\pi} \ln \csc \frac{\pi}{2} \frac{d}{D} \right\}. \tag{19}$$

In expression (19), the higher order correction terms to the ln csc functions have been neglected. The final step is to arrange expression (19) into a form more suitable for solution and discussion.

Define

$z = x + jy = \gamma_0 b$;
$h = b/a$, ratio of transmission waveguide height to width;
$\theta = 2a/\lambda$, ratio of transmission waveguide width to one half the free-space wavelength;
$\epsilon = L/a$, ratio of slot period to waveguide width;
$\sigma = d/L$, ratio of slot width to slot period;
$\delta = D/L$, ratio of side waveguide height to slot period. (20)

Expression (19) then becomes

$$\frac{\coth z}{z} \approx -\frac{1}{\pi h} \left\{ \frac{\delta^{-1}}{\sqrt{1-\theta^2}} + \epsilon \left[\ln \csc \frac{\pi}{2} \sigma + \ln \csc \frac{\pi}{2} \frac{\sigma}{\delta} \right] \right\}$$
$$= w = -u + jv. \tag{21}$$

The normalized propagation constant $(\gamma_z a)$ is given by

$$\gamma_z a = \alpha a + j\beta a = \pi \sqrt{1 - \theta^2 - \left(\frac{z}{\pi h} \right)^2}. \tag{22}$$

Discussion of Transverse Resonance Equation

Eq. (21) is a complex transcendental equation. For a given θ, there exist an infinite number of solutions. Each solution, however, lies on a separate Riemann sheet, and hence, corresponds to a distinct leaky-wave mode. We will be concerned with the least attenuated mode for θ varying from 0 to 2. This mode corresponds to solutions on the first Riemann sheet, or for values of y lying between 0 and $\pi/2$.

It can be shown that the complex function $w = \coth z/z$ carries any second quadrant vector z that lies in or on the boundary of the shaded region of Fig. 3[14] into the second quadrant (including the axis') of the w plane. An examination of (21) shows that the right-hand side is either negative real (for $\theta < 1$) or complex (for $\theta > 1$) having values in the second quadrant. Hence, the solutions of (21) lie in the shaded region of Fig. 3; their extremes are established by the boundaries of the region. They are

$$0 \le |x| \le 0.600 \text{ (approximately)}$$
$$0 \le y \le \pi/2. \tag{23}$$

Solutions of (21), for specific values of the parameters and of the frequency variable θ, were obtained by use of a medium-speed electronic computer. The method of solution was to use an iterative equation based on Newton's method[15] as applied to real functions of a

[12] An investigation of the range of parameters and frequency for which the approximations (9) and (16) remain valid is contained in "Suppression of Spurious Frequencies," Stanford Research Inst., Menlo Park, Calif., E. G. Cristal, L. Young, and B. M. Schiffman, Quart. Prog. Rept. No. 3, Project No. 4096, Contract No. AF 30(602)-2734; January, 1963. For the frequency interval reported in this paper, the approximations were generally good.

[13] R. E. Collin, *op. cit.*, pp. 338–348.

[14] It can be demonstrated by substitution into coth z/z that the positive imaginary axis of the z plane from 0 to $\pi/2$ maps into the negative real axis of the w plane, and that the curved boundary line of Fig. 3 given by solutions of the equation

$$x \sinh 2x = y \sin 2y \quad \text{for } x, y \ne 0 \quad \text{and} \quad x < 0; \quad 0 \le y \le \pi/2$$

maps into the imaginary positive axis of the w plane.

[15] R. Courant, "Differential and Integral Calculus," Interscience Publishers, Inc., New York, N. Y., vol. 1, pp. 355–359; 1952.

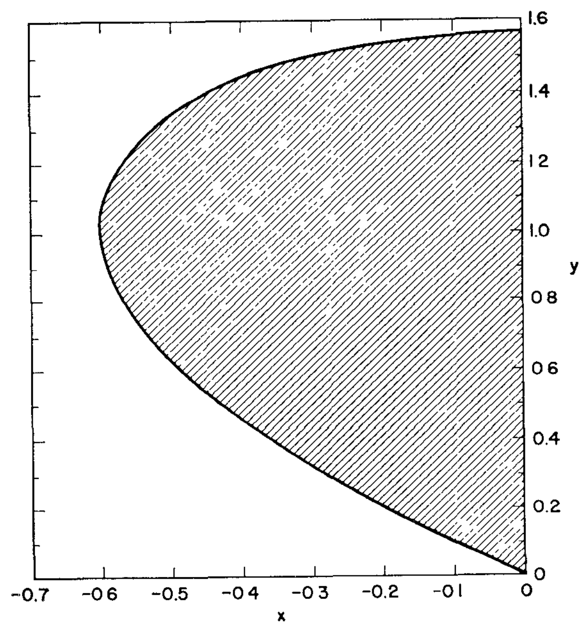

Fig. 3—Section of the first Riemann sheet showing the region of solutions of

$$\frac{\coth z}{z} = -u + jv(u, v \geqq 0).$$

complex variable. Convergence was found to be very rapid. The basic iterative equation is as follows:

$$z_{i+1} = \frac{\coth z_i + z_i \operatorname{csch}^2 z_i}{w + \operatorname{csch}^2 z_i}, \qquad \text{for } i = 1, 2, \cdots. \tag{24}$$

Discussion of Results

In order to investigate the dependence of the attenuation constant on the several design parameters and frequency, (21) was solved as a function of θ for various values of ϵ, σ, δ, h. The following cases, which assume a waveguide of fixed width a, were of particular interest:

1) For a given slot period ϵ, slot width σ and main waveguide height h determine the dependence of the attenuation constant on the absorbing waveguide height δ.
2) For a given slot period ϵ, absorbing waveguide height δ and main waveguide height h determine the dependence of the attenuation constant on the slot width σ.
3) For a given slot period ϵ, absorbing waveguide height δ and slot width σ determine the dependence of the attenuation constant on the main waveguide height h.
4) For a given slot width σ, absorbing waveguide height δ and main waveguide height h determine the dependence of the attenuation constant on the slot period ϵ.

The graphs of Figs. 4 through 9 pertain to Cases 1 through 4. They have plotted αa, the normalized attenuation constant, vs $2a/\lambda$, the ratio of waveguide width to one half the free-space wavelength. The region $0 \leq 2a/\lambda \leq 1$ is that of nonpropagation in an unperturbed guide, *i.e.*, $\beta = 0$. For the leaky-wave structure of Fig. 2, this frequency region also corresponds to nonpropagation. However, the value of the normalized attenuation constant αa was found to be increased over that of the unperturbed case. The region $1 < 2a/\lambda < \infty$ corresponds to the region of propagation in an unperturbed waveguide, *i.e.*, $\beta > 0$, $\alpha = 0$. For the leaky-wave structure of Fig. 2, β was found to be slightly more than the unperturbed waveguide value for θ less than approximately 1.2, and slightly less than the unperturbed value for θ greater than approximately 1.2, while α differed from zero. The variation of α with frequency and its dependence on ϵ, σ, δ and h will now be discussed.

Figs. 4, 5 and 6 relate to Cases 1 and 2. Fig. 4 considers the example of the slot width occupying 25 per cent of the slot period, Fig. 5 the case of the slot width occupying 50 per cent of the slot period and Fig. 6 the case of the waveguide periodic E plane T junction (*i.e.*, $\sigma = \delta$). In all three cases, δ, the ratio of the absorbing waveguide height to the slot period, is a variable parameter that ranges from the minimum permissible value to the limiting value 1. The theoretical results obtained suggest the following conclusions:

1) The attenuation constant increases as the absorbing waveguide height increases. A fair approximation to the dependence of αa on δ for the maximum values of αa is

$$\frac{(\alpha a)_1}{(\alpha a)_2} \approx \frac{\delta_1}{\delta_2}. \tag{25}$$

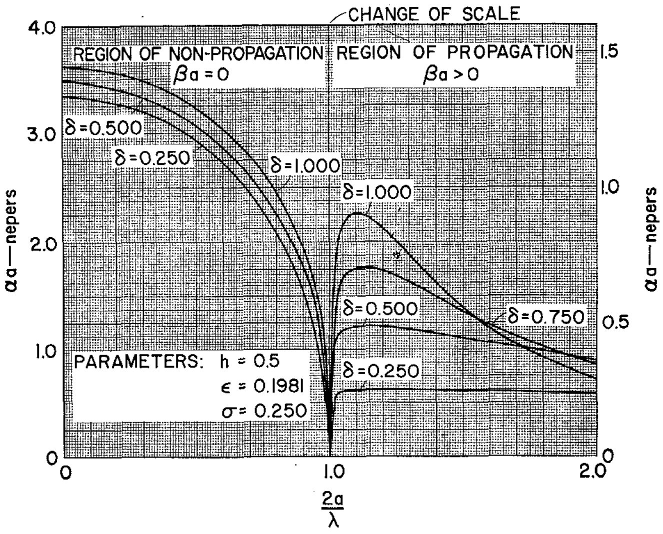

Fig. 4—Normalized attenuation constant αa as a function of $2a/\lambda$ for various values of $\delta(\sigma=0.250)$.

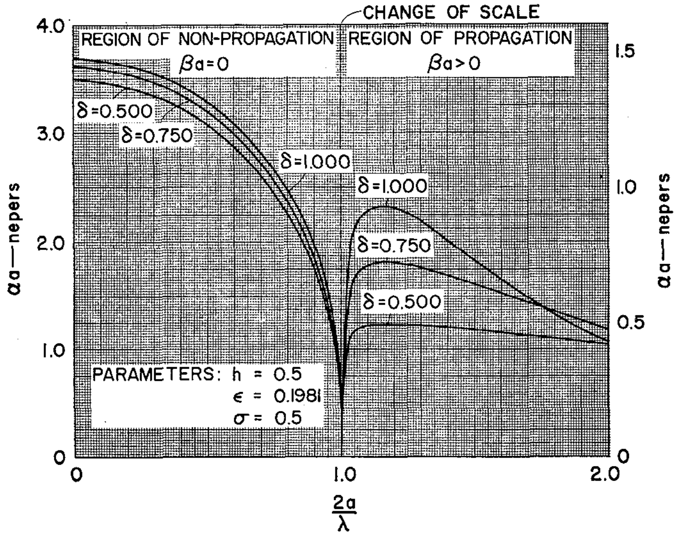

Fig. 5—Normalized attenuation constant αa as a function of $2a/\lambda$ for various values of $\delta(\sigma=0.500)$.

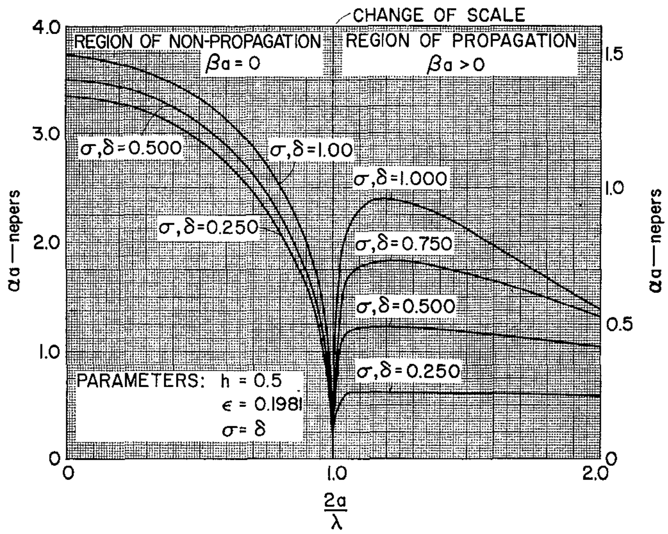

Fig. 6—Normalized attenuation constant αa as a function of $2a/\lambda$ for various values of σ and $\delta(\delta=\sigma)$.

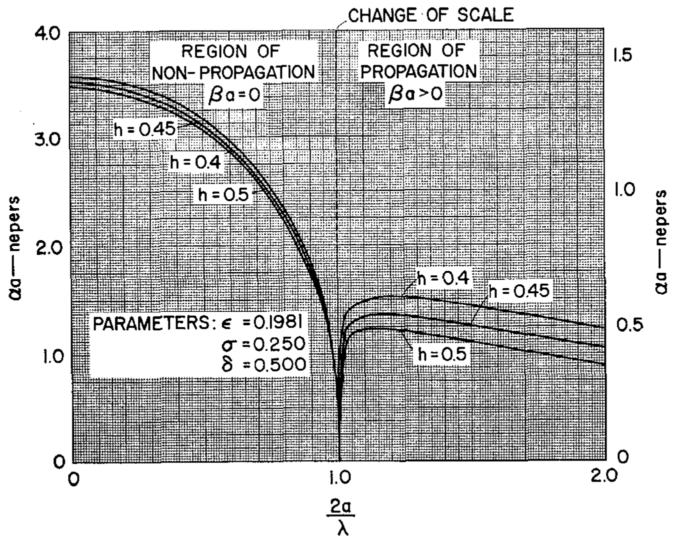

Fig. 7—Normalized attenuation constant αa as a function $2a/\lambda$ for various values of $h(\sigma=0.250,\ \delta=0.500)$.

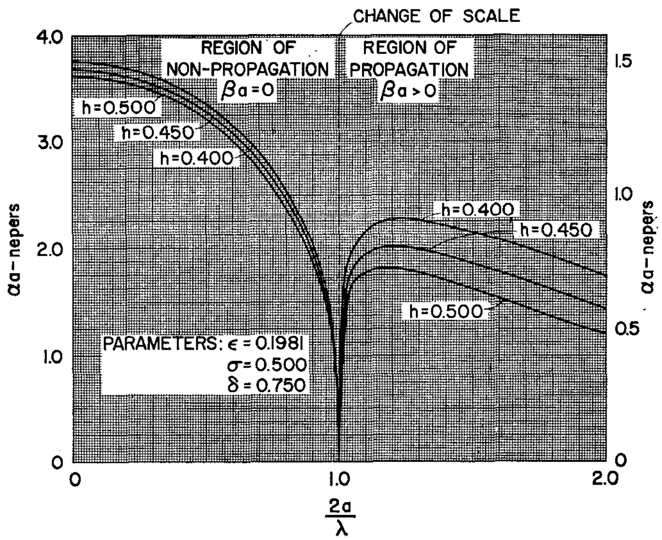

Fig. 8—Normalized attenuation constant αa as a function of $2a/\lambda$ for various values of $h(\sigma=0.500,\ \delta=0.750)$.

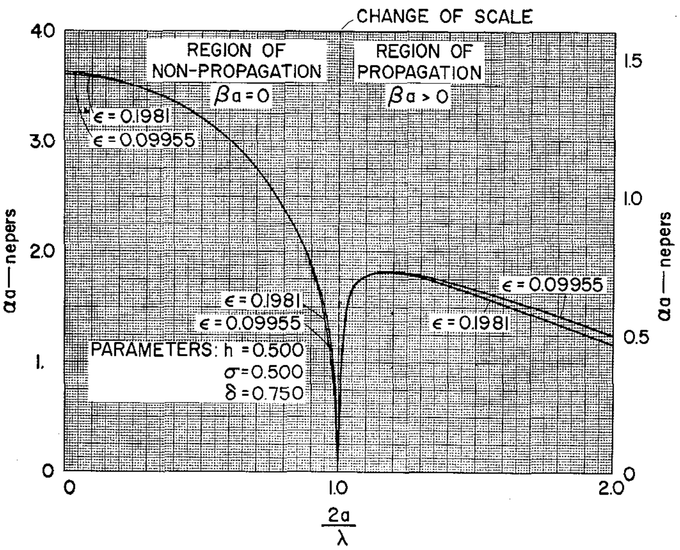

Fig. 9—Normalized attenuation constant αa as a function of $2a/\lambda$ for various values of $\epsilon(\sigma=0.500,\ \delta=0.750)$.

2) The frequency sensitivity of αa increases as the absorbing waveguide height increases. Whereas over most of the frequency band the absolute value of the slope of the αa vs θ curves is relatively small for small values of δ, it increases monotonically with increasing δ. For a given σ, the least-frequency-sensitive case is when $\delta=\sigma$, *i.e.*, the waveguide periodic T junction.

Figs. 7 and 8 show the effect upon the attenuation constant of varying the main waveguide height while holding all other parameters constant. The particular cases shown are $\sigma=0.250$, $\delta=0.500$ and $\sigma=0.500$, $\delta=0.75$; however, the results are quite similar for the other cases investigated. The effect of reducing the waveguide height is to increase the attenuation constant without affecting its frequency sensitivity. This particular result has been experimentally verified in the case of coaxial leaky-wave filters[12] where the inner conductor diameter was increased, thus reducing the line impedance and has also been noted in the waveguide case.[3] For the range of parameters investigated in this work, an approximate relationship between various h curves was found to be

$$\frac{(\alpha a)_2}{(\alpha a)_1} = c\left(\frac{h_1}{h_2}\right); \qquad (h_2 < h_1) \tag{26}$$

where c varied from 1 to 1.3.

Fig. 9 shows the effect of varying the slot period holding all other ratios constant. The change in αa due to the variation in ϵ is relatively small throughout most of the frequency band but reaches a maximum of 6 per cent at $\theta=2.0$. The example represented by Fig. 9 considers reducing the slot period by 50 per cent. In most leaky-wave filters, this is about the practical limit of period reduction. Fig. 9 shows that the smaller period tends to slightly increase α and to slightly reduce its frequency sensitivity; however, this advantage is completely offset by the additional number of absorbing waveguides (double for this example) required by the reduction in the slot period.

In the Introduction it was stated that the analysis presented in this paper could be easily extended to include the case of slots on both broad walls. This extension is made for a given set of parameters ϵ, σ, δ and h by replacing h of that set by $h/2$ and solving (21) and (22). This is physically equivalent to placing a conducting wall in the H plane at the half-height position of the main waveguide. Assuming that the approximations made in the derivation of (21) are then not invalidated, one sees that, qualitatively, all of the results of this study remain unchanged for the case of the leaky-wave waveguide structure with slots on both broad walls.

Experimental Work

Referring to Fig. 2(b), denote an arbitrary absorbing waveguide as the ith guide and any subsequent absorbing waveguide as the jth guide ($j>i$). Then the ratio of power in the ith guide to power in the jth guide is given by

$$\frac{P_i}{P_j} = e^{2(\alpha a)\epsilon(j-i)}. \tag{27}$$

Solving (27) for αa gives

$$\alpha a = \frac{1}{20\epsilon(j-i)\log_{10} e}\left\{10 \log_{10}\frac{P_i}{P_j}\right\}. \tag{28}$$

Eq. (28) states that αa is equal to the difference in db of the power in the jth and ith guides divided by $8.68(j-i)\epsilon$.

Using (28) to calculate αa, experimental measurements were made on a waveguide structure that was designed so that it could be easily modified to incorporate the following four cases:

CASE I	CASE II
$\epsilon = 0.198$	$\epsilon = 0.198$
$h = 0.472$	$h = 0.428$
$\sigma = \delta = 0.555$	$\sigma = \delta = 0.555$
CASE III	CASE IV
$\epsilon = 0.198$	$\epsilon = 0.198$
$h = 0.465$	$h = 0.421$
$\sigma = 0.200$	$\sigma = 0.200$
$\delta = 0.555$	$\delta = 0.555$

The power in several absorbing waveguides was measured and the value of αa was then calculated by (28) using several combinations for j and i of the absorbing waveguides. Since the resulting αa values varied slightly for different values of j and i, their average value is used in the final result. The variation of the αa values that were calculated from the power measurements results from the variation of VSWR of the loads in the side waveguides. A check of several loads showed that the VSWR's varied from 1.05 to 1.35 over the measured frequency interval. Hence, because of the reflections caused by these loads the coupling varied slightly from guide to guide.

Fig. 10 gives the computed and measured values of αa for the case of the periodic T junction for two values of main waveguide height. Fig. 11 gives the results for the case where the slot width occupies 20 per cent of the slot period for two values of waveguide height. In the latter case, the slot thickness was 0.003 inch and the small thickness correction term was neglected in the theoretically computed values of αa. The additional 0.004-inch reduction in height (compare h in Figs. 10 and 11) resulted from the particular fabrication technique used in attaching the slot strips to the end of the absorbing waveguides. The four experimental cases give good agreement with the theoretically computed values.

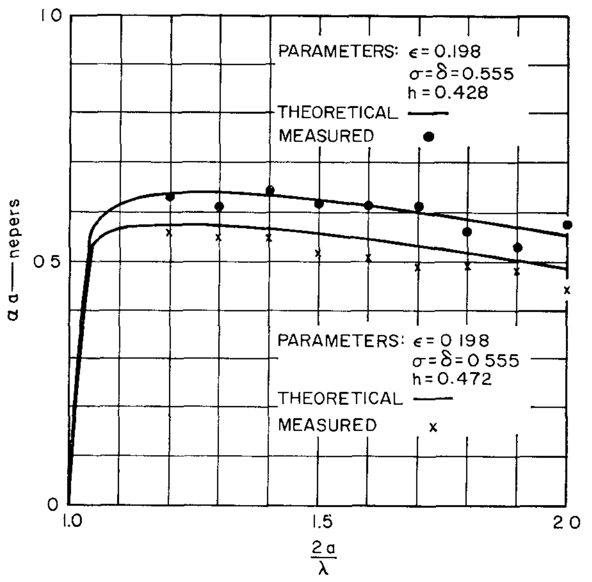

Fig. 10—Theoretically computed and experimentally measured normalized attenuation constant αa as a function of $2a/\lambda$ for two values of $h(\epsilon=0.198, \sigma=\delta=0.555)$.

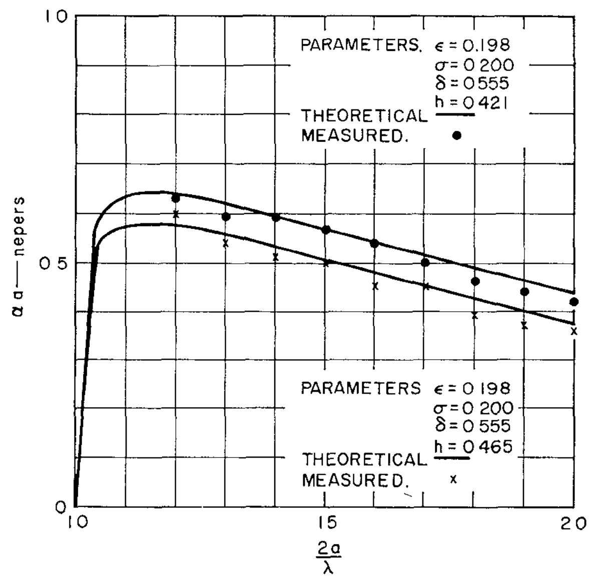

Fig. 11—Theoretically computed and experimentally measured normalized attenuation constant αa as a function of $2a/\lambda$ for two values of $h(\epsilon=0.198, \sigma=0.200, \delta=0.555)$.

Conclusions

An analysis of a waveguide leaky-wave filter structure over a limited frequency range has shown how the normalized attenuation constant (*i.e.*, the attenuation constant per unit length multiplied by the main waveguide width) depends on various design parameters. The dependence of the attenuation constant upon these parameters may be expected to follow the same general pattern for waveguide leaky-wave filters attenuating incident TE_{10}-mode energy. For the case of incident TE_{n0} modes $(n>1)$, the analysis should also provide useful quantitative design data.

The results of the analysis are summarized in the following statements:

1) The peak value of the normalized attenuation constant is approximately directly proportional to the absorbing waveguide height and also to the coupling slot width. For the range of design parameters investigated, the constant of proportionality varied only slightly.
2) The frequency sensitivity of the normalized attenuation constant increases with increasing height of the absorbing waveguide.
3) For a given slot width, the periodic T junction is the least-frequency-sensitive filter configuration.
4) The normalized attenuation constant is approximately inversely proportional to the main waveguide height. For the range of design parameters investigated the constant of proportionality was found to vary up to approximately 30 per cent.
5) The attenuation per unit length is very insensitive to small changes in the slot period. Thus, increasing the number of slots per unit length is not an effective method of increasing the attenuation of the filter. However, there is a tendency to increase the attenuation per unit length very slightly for smaller slot periods.

Acknowledgment

The experimental waveguide leaky-wave filter was constructed by J. Culich and R. Pierce. V. Sagherian programmed the Burroughs 220 Computer. P. Reznek took most of the experimental data.